Experimental observation of the Dzyaloshinskiĭ-Moriya electron-nuclear interaction by the electron-nuclear double resonance method

A. I. Rokeakh, A. S. Moskvin, N. V. Legkikh, and Yu. A. Sherstkov

A. M. Gorki Ural State University, Sverdlovsk

(Submitted 30 October 1986)
Zh. Eksp. Teor. Fiz. **93**, 1789-1799 (November 1987)

The electron-nuclear double resonance method (ENDOR) was used to study an indirect hyperfine interaction (IHFI) of Gd^{3+} impurity ions with ^{207}Pb nuclei in ferroelectric $Pb_5Ge_3O_{11}$. An antisymmetric Dzyaloshinskiĭ-Moriya electron-nuclear interaction was observed and investigated for the first time. An explanation of its magnitude, comparable in the present case with the symmetric IHFI, was based on a mechanism of electric and magnetic polarization of $^{207}Pb^{2+}$ ions resulting from the IHFI, because of a strong $6sp$ hybridization and a large magnitude of the spin-orbit interaction in the electron shell of these ions. The relationship between the magnitude of the isotropic IHFI and the geometry of the exchange coupling in the Gd^{3}–O^{2}–Pb^{2+} chain was analyzed.

I. INTRODUCTION

Theoretical and experimental investigations of hyperfine interactions (HFI) are among the most important methods for the study of the electron structure of matter, charge and spin density distributions, electric polarization, crystal structure, magnetic ordering and their changes due to various external agencies, phase transitions, substitutions, etc. Effective techniques for the investigation of HFIs are the magnetic resonance methods, particularly electron spin resonance (ESR) and electron-nuclear double resonance (ENDOR).

The application of these methods to the investigation of low-symmetry paramagnetic complexes, and the high precision (particularly that characteristic of ENDOR) make it necessary to provide a satisfactory description of all the characteristics of the experimental spectra of what is known as the generalized spin Hamiltonian,[1] a part of which describing the HFI linear in the spins S and I is

$$\mathscr{H}_{\mathrm{HFI}} = \mathscr{H}^{(0)}_{\mathrm{HFI}} + \mathscr{H}^{(1)}_{\mathrm{HFI}} + \mathscr{H}^{(2)}_{\mathrm{HFI}}, \tag{1}$$

where

$$\mathscr{H}^{(0)}_{\mathrm{HFI}} = A_0 \mathbf{SI} \tag{2}$$

is the Hamiltonian of the isotropic HFI (A_0 is a scalar),

$$\mathscr{H}^{(1)}_{\mathrm{HFI}} = \mathbf{A}_1[\mathbf{SI}] \tag{3}$$

is the Hamiltonian of the antisymmetric hyperfine interaction ($\mathbf{A}_1$ is the axial vector),

$$\mathscr{H}^{(2)}_{\mathrm{HFI}} = \hat{A}_2[\hat{S}^{(1)} \otimes \hat{I}^{(1)}]^{(2)} \tag{4}$$

is the Hamiltonian of the symmetric HFI ($\hat{A}_2$ is a symmetric zero-trace tensor of rank 2).

The antisymmetric HFI described by $\mathscr{H}^{(1)}_{\mathrm{HFI}}$ is an electron-nuclear analog of the familiar Dzyaloshinskiĭ-Moriya interaction[2,3]

$$\mathscr{H}_{\mathrm{DM}} = \mathbf{D}_{12}[\mathbf{S}_1\mathbf{S}_2],$$

which is one of the main interactions governing the magnetic structure, as well as magnetic, magnetooptic, resonance, and several other properties of a wide range of magnetic materials (weak ferromagnets). In the case of these compounds the symmetry admits also the existence of electron-nuclear invariants of the type described by Eq. (3). The electron-nuclear Dzyaloshinskiĭ-Moriya interaction in weak ferromagnets and ways of detecting it experimentally were first discussed by Ozhogin.[4]

Means for observing the effects of the anti-symmetry of rank-2 tensors $\hat{g}$ and $\hat{A}$ in ESR and of a tensor σ representing magnetic screening of the nuclei in NMR in magnetically dilute compounds have also been considered some time ago.[5,6] However, the antisymmetric components of $\hat{g}$, $\hat{A}$, and $\hat{\sigma}$ have not yet been detected by a magnetic resonance method.

The difficulties encountered in the experimental detection of the antisymmetric components of the electron-nuclear interaction are related primarily to the fact that they make no first-order contribution to the energy of the electron-nuclear system and are allowed only if the crystal symmetry is less than orthorhombic. Moreover, in some cases (particularly in the case of rare-earth ions with nonzero orbital momenta),[7,8] the true spin antisymmetry of the HFI can be identified as the antisymmetry in the space of fictitious spin of Stark levels. In fact, an allowance for the crystal field in the $[SL]J$ scheme [$4f$ ions with are not in the S state) and introduction of a fictitious angular momentum $\mathbf{j}$ of a Stark sublevel (as shown, for example, by Levy in a similar situation)[9] may result in an effective antisymmetry of the HFI even due to symmetric contributions.

We shall report experimental observations, by the ENDOR method, of the effects of the true antisymmetry of the tensor representing the indirect hyperfine interaction (IHFI) of Gd^{3+} ($4f^7$, $^8S_{7/2}$) ions with one of the structure types of ^{207}Pb nuclei in a crystal of lead germanate ($Pb_5Ge_3O_{11}$).

2. EXPERIMENTS

The ENDOR spectra of Gd^{3+} impurity centers in a $Pb_2Ge_3O_{11}$ crystal were recorded at liquid helium temperature. A ferroelectric distortion of the lattice at this temperature was responsible for a large number of structurally inequivalent positions of the ^{207}Pb nuclei, including those with a low symmetry (C_1). Preliminary results of investigations of the IHFI of the Gd^{3+} impurity ions with the nearest ^{207}Pb

 0038-5646/87/111021-07$04.00

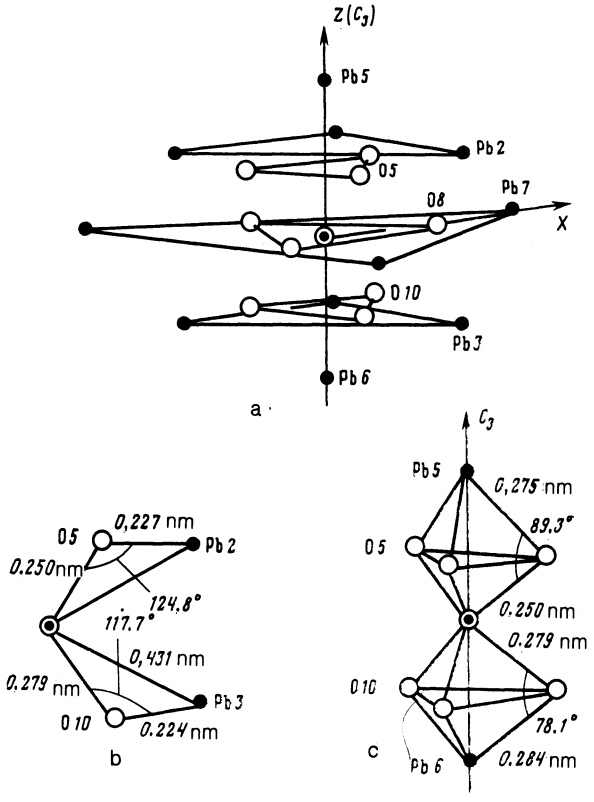

FIG. 1. a) Immediate environment of a Gd^{3+} impurity ion (at the Pb4 position) in lead germanate. b), c) Structure of IHFI chains for nonaxial (b) and axial (c) ^{207}Pb nuclei: the open circles denote O^{2-}, the black dots denote Pb^{2+}, and a circle with a dot represents Gd^{3+}.

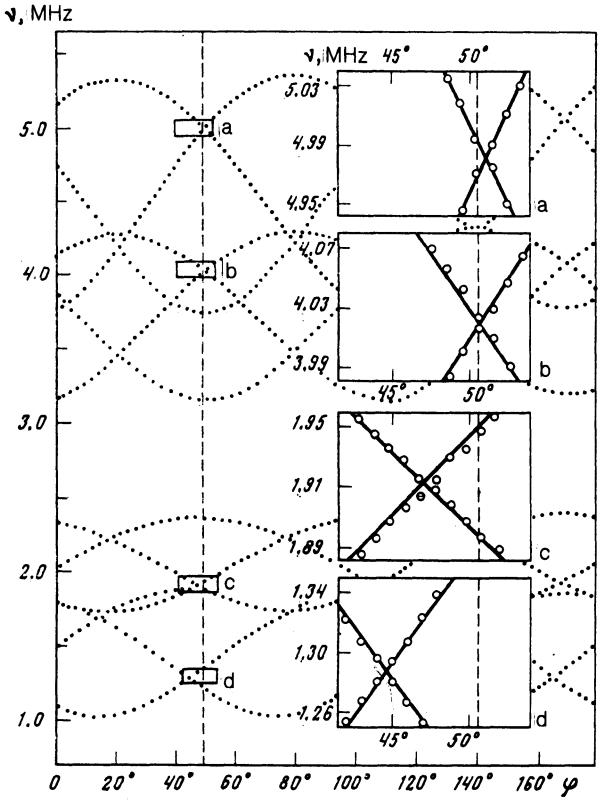

FIG. 2. Azimuthal angular dependences of the ENDOR frequencies of the ^{207}Pb nuclei (type I) plotted for some projections of the electron spin: a) $\tilde{M} = -3.434$ ($\approx -7/2$) and b) $\tilde{M} = -2.375$ ($\approx -5/2$) in a field $B = 206.3$ mT; c) $\tilde{M} = 1.513$ ($\approx 3/2$) and d) $\tilde{M} = 2.446$ ($\approx 5/2$) in $B = 357.5$ mT; the points are the experimental values and the continuous curves are calculated.

nuclei in this crystal were published earlier.[10] The results of this investigation demonstrated that the ferroelectric phase was characterized by a considerable difference between the isotropic IHFI of the nuclei (those on the trigonal axis of impurity centers and off this axis) occupying enantiomorphic positions, equivalent in respect of the IHFI, in the paraelectric phase.

The symmetry of the positions of the ^{207}Pb nuclei closest to the impurities, denoted by Pb2 and Pb3-C_1 in Fig. 1, admits the existence of antisymmetric components in the IHFI tensor.[11] A careful investigation of the azimuthal angular dependences of the ENDOR frequencies of these nuclei in an external magnetic field H oriented at right-angles to the trigonal axis of the crystal revealed characteristic features of one of them identified in Ref. 10 as I. These features were manifested by a considerable difference between the positions of extrema of the angular dependences of both different ESR transitions and different electronic states within one transition (the scatter of the positions of these extrema between the twelve investigated angular dependences exceeded 7°).

Figure 2 shows, by way of illustration, the experimentally determined angular dependences of the ENDOR frequencies recorded in the $H \perp C_3$ case for two ESR transitions. The relative shift of the angular dependences was manifested most clearly in the region of intersection of the branches of the dependence associated with three ^{207}Pb nuclei in a structure of type I located at the vertices of an equilateral triangle with its center on the C_3 axis. These regions (a, b, c, d) are shown on an enlarged scale in Fig. 2. In view of the small line width ($\lesssim 20$ kHz) the positions of the points of intersection of the branches of the dependence were determined with an error not exceeding 0.5° (Fig. 3). In the present study we concentrated our attention on the characteristics of the IHFI of this particular type of structure of the nuclei.

The observed dependences cannot be explained by an axial model of the interaction and cannot be attributed to some accidental experimental errors. The main source of

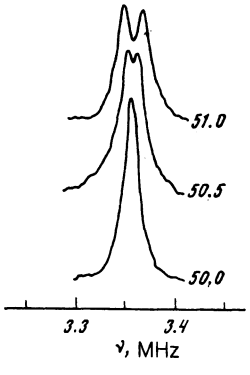

FIG. 3. Form of the spectrum in the region of intersection of the azimuthal angular dependences of the ENDOR frequencies two crystallographically equivalent ^{207}Pb nuclei (type I) $B = 265.5$ mT, $M = -3/2$, and the numbers alongside the spectra give the angle φ in degrees.

such errors is a possible deviation of the orientation of the C_3 axis of a sample in the process of recording the relevant dependences. However, a deliberate controlled misorientation of the C_3 axis relative to the axis of rotation of the applied magnetic field showed that errors of this kind could not account for the observed mutual shifts of the extrema of the aximuthal angular dependences.

Therefore, the different positions of the extrema of the azimuthal dependences of the ENDOR frequencies belonging to the same ^{207}Pb nuclei (structure type I) were a reflection of the characteristics of the IHFI between the impurity ions and these particular nuclei, and required a theoretical description with retention of the relevant terms in the generalized spin Hamiltonian.

3. PHENOMENOLOGICAL THEORY

We shall restrict our analysis to the case of the IHFI of a paramagnetic ion with a single nucleus (assuming that the nuclear-nuclear interaction is negligible). Then the spin Hamiltonian of the electron-nuclear system is

$$\mathcal{H}=\mathcal{H}_0+\mathcal{H}_{\text{IHFI}}+\mathcal{H}_n, \tag{5}$$

where $\mathcal{H}_0$ contains terms representing the fine structure and the interaction of the electron spin of Gd^{3+} with an external magnetic field, $\mathcal{H}_n$ is the nuclear Zeeman interaction, and $\mathcal{H}_{\text{IHFI}}$ is the indirect hyperfine interaction of a paramagnetic ion with a lead nucleus, which is not subject to any restrictions as regards the symmetry.

The ENDOR frequencies can be found, allowing for the smallness of $\mathcal{H}_{\text{IHFI}}$ and $\mathcal{H}_n$ compared with $\mathcal{H}_0$, by diagonalization of the Hamiltonian $\mathcal{H}_{\text{ENDOR}}$ containing only the nuclear variables:

$$\mathcal{H}_{\text{ENDOR}}=\sum_{i,k}^{3}\{\tilde{M}_iA_{ik}I_k-\gamma_{ik}H_iI_k\delta_{ik}\}, \tag{6}$$

where $\tilde{M}_i=\langle\Psi_n|S_i|\Psi_n\rangle$ is the effective projection of the electron spin in the n-th state of $\mathcal{H}_0$; A_{ik} is the tensor describing the IHFI; $\gamma_{ik}=g_{ik}\beta_n$; g_{ik} is the nuclear g tensor; H_i and I_k are, respectively, the components of the external magnetic field and the nuclear spin ($I=\frac{1}{2}$ for ^{207}Pb).

A general tensor $\hat{A}$ corresponding to the C_1 symmetry has the following form in the system of principal axes of the symmetric part of this tensor:

$$\hat{A}=A_s\begin{pmatrix}1&0&0\\0&1&0\\0&0&1\end{pmatrix}-A_p\begin{pmatrix}1+\eta&0&0\\0&1-\eta&0\\0&0&-2\end{pmatrix}+\begin{pmatrix}0&-a_3&a_2\\a_3&0&-a_1\\-a_2&a_1&0\end{pmatrix}, \tag{7}$$

where

$$A_s=(A_{xx}+A_{yy}+A_{zz})/3,$$
$$A_p=(A_{zz}-A_s)/2,\quad \eta=(A_{yy}-A_{xx})/2A_p.$$

The parameters A_s and A_p represent the axial interaction and correspond to the generally accepted definition of Ref. 12, η is a parameter representing the nonaxial behavior, and the third term in Eq. (7) corresponds to the antisymmetric part of the IHFI.

It therefore follows from Eq. (7) that the IHFI tensor for the symmetry group C_1 contains six parameters A_s, A_p, η, a_1, a_2, and a_3, corresponding to specific components of the interaction with particular symmetries. The missing three parameters (the total number of parameters of C_1 is nine) are the three Euler angles α, β, and γ which transform the system of principal axes into the laboratory coordinate system.

The azimuthal angular dependences obtained in the $H\perp C_3$ case for the square of the frequency of the ENDOR signals due to the ^{207}Pb nuclei in $Pb_5Ge_3O_{11}$, when the spectrum of this compound is described by the spin Hamiltonian $\mathcal{H}_0$ with the C_{3v} symmetry (Ref. 10), can be represented as a Fourier series[11]:

$$\nu_\perp^2=\bar{A}_0+\sum_{n=1}^{3}\bar{A}_{2n}\cos 2n\varphi+\sum_{n=1}^{3}\bar{B}_{2n}\sin 2n\varphi. \tag{8}$$

The fourth and sixth harmonics in Eq. (8) originate from an interaction of the S^3I type, an allowance for which may be essential for the satisfactory description of the ENDOR spectrum. The same S^3I interaction contributes also to the magnitudes of the remaining harmonics.

Analytic expressions for the squares of the ENDOR frequencies in the $H\|C_3$ case and of the amplitudes of the harmonics of the expansion (8) can be expressed in terms of a set of intermediate parameters λ_j which are known functions of the IHFI parameters and of the Euler angles of a given nucleus and are independent of the projections of the electron spin $\hat{M}_i$ and of the external magnetic field H which occur explicitly in the expressions:

$$\nu_\|^2=\tilde{M}_\|^2\lambda_1+\tilde{M}_\|H_\|\lambda_2+H_\|^2\lambda_3+[5\tilde{M}_\|^3-\{3S(S+1)-1\}\tilde{M}_\|]\times(\tilde{M}_\|\lambda_{11}+H_\|\lambda_{12}), \tag{9}$$

$$\bar{A}_0=\tilde{M}_\perp^2\lambda_4+\tilde{M}_\perp H_\perp\lambda_5+H_\perp^2\lambda_6+[5\tilde{M}_\perp^3-\{3S(S+1)-1\}\tilde{M}_\perp](\tilde{M}_\perp\lambda_{13}+H_\perp\lambda_{14}), \tag{10}$$

$$\bar{A}_2=\tilde{M}_\perp^2\lambda_7+\tilde{M}_\perp H_\perp\lambda_8+[5\tilde{M}_\perp^3-\{3S(S+1)-1\}\tilde{M}_\perp](\tilde{M}_\perp\lambda_{15}+H_\perp\lambda_{16}), \tag{11}$$

$$\bar{B}_2=\tilde{M}_\perp^2\lambda_9+\tilde{M}_\perp H_\perp\lambda_{10}+[5\tilde{M}_\perp^3-\{3S(S+1)-1\}\tilde{M}_\perp)\times(\tilde{M}_\perp\lambda_{17}+H_\perp\lambda_{18}). \tag{12}$$

The contributions of the fourth and sixth harmonics of Eq. (8) are not included because they are not used in an analysis of the experimental results. The parameters λ_{11}-λ_{18} vanish in the absence of an interaction of the S^3I type. The explicit form of the parameter λ_j can be found in Ref. 11.

The procedure for the determination of the required IHFI parameters and Euler angles from the ENDOR spectra thus divides into three relatively independent stages:

1) expansion of the azimuthal angular dependences $\nu_1^2(\varphi)$ as Fourier series of the type given by Eq. (8) and determination of the amplitudes of the harmonics;

2) determination of the parameters λ_1-λ_{18} representing the IHFI of the investigated nuclei by solving overdetermined linear systems (9)–(12);

3) determination of the IHFI parameters A_s, A_p, η, a_1, a_2, α, β, and γ from a linear system of equations governing the relationship between the IHFI parameters and λ_j.

TABLE I. Structure and IHFI parameters of ^{207}Pb nuclei closest to Gd^{3+}

Nucleus	A_s, kHz	A_p, kHz	η	α, deg	β *, deg	γ, deg	Comments
I	725.6(8) **	180.1(6)	0.093(22)	−36.5(27)	65.8(1)	42.0(2)	$a_1=-19(7)$ kHz $a_2=-112(5)$ kHz $a_\perp=-0.5(7)$ kHz $a_\parallel=-2.5(14)$ kHz
II	5.7(28)	211.4(31)	0.07(6)	0,0	66.4(3)	37.0(5)	–
III	−33.5(20)	81.0(12)	0.0	0,0	81.0(20)	0	$\gamma=0$ by definition
IV	−1476.3(24)	203.5(13)	–	–	0.0	–	$a_\parallel=0.23(6)$ kHz
V	≈−400	≈200	–	–	0.0	–	see Ref. 10

*The smallest angles between the z axis of the system of principal axes of the nucleus, on the one hand, and the axis C_3, on the other are given. **The values in parentheses represent the error in units of the lowest digit of the listed value.

The parameter a_3 representing the antisymmetric part of the IHFI does not occur in our expressions for the frequency and, consequently, it cannot be determined.

4. EXPERIMENTAL RESULTS AND DISCUSSION

The parameters λ_1-λ_{18} of the nuclei with the type I structure were found by solving three overdetermined linear equations [Eqs. (9) and (10) simultaneously, and Eqs. (11) and (12)] by the singular expansion (SVD) method.[13] The results of a numerical analysis of the systems (9)–(12) show that it is necessary to include terms of the S^3I type and a singular analysis of the solution demonstrates that complication of the model by inclusion of additional fitting parameters is within the range of precision of the experimental results accurate to within 2–3 kHz.

The eight required parameters of the IHFI of the nuclei with the type I structure were determined from a known set of parameters λ_1-λ_{10} by solving a system of eight nonlinear equations. A numerical analysis of the system demonstrated the existence of a single unique solution given in Table I. The set of the IHFI parameters found in this way corresponded to the symmetry of the interaction and, within the limits of the experimental error, described the ENDOR spectra in the $H \| C_3$ and $H \perp C_3$ cases. An attempt to describe the ENDOR spectra on the assumption that the symmetry of the interaction is C_3 (or C_2 or C_{2v}), which corresponds to the solution of the nonlinear system in the case when $a_1 = a_2 = 0$, was unsuccessful. Consequently, the set of the IHFI parameters listed in Table I is the only set that provides a satisfactory description of the experimental results. The parameters $a_\parallel$ and $a_\perp$ (see Ref. 11) representing the axial component of the interaction of the S^3I type were found from the values of $\lambda_{11} - \lambda_{18}$.

The quality of the description of the experimental results achieved in this way is illustrated in Fig. 2, where the continuous curves are the theoretical dependences plotted using the parameters listed in Table I. The vertical dashed line represents the positions of intersections of the theoretical dependences in the case when the nonaxial part of the IHFI tensor vanishes.

The ENDOR spectra of the nuclei denoted by II in Ref. 10 and occupying in the paraelectric phase a position, which is mirror-symmetric relative to the nuclei of type I, failed to reveal differences between the positions of the extrema. However, it was possible to describe these spectra (within the limits of the experimental error) only on the assumption that the IHFI symmetry is C_s (or C_2 or C_{2v}), which can be seen from Table I. The nuclei of type III occupy the Pb7 positions on the assumption that Gd^{3+} occupies the Pb4 positions, and all the more distant nuclei are described by the axial IHFI. Table I gives also the IHFI parameters of two axial ^{207}Pb nuclei closest to Gd^{3+} and occupying the Pb5 and Pb6 positions (local symmetry C_3) identified by IV and V.

According to Ref. 14, the antisymmetric interaction of the $\mathbf{A}_1$ [S·I] type appears in the second order of perturbation theory as a result of simultaneous effects of the spin-orbit interaction V_{so} of the paramagnetic ions and of the IHFI in the M–O–N plane (M is a paramagnetic ion, N is the investigated nucleus, and O is an intermediate nonmagnetic ion). However, this mechanism is ineffective in the case of the $^8S_{7/2}$ ions, because the spin-orbit interaction of these ions is easily diagonalized by a transition to the $[SL]J$ scheme (when the SL mixing is allowed), which simply results in a small admixture of the excited $^6P_{7/2}$ and $^6D_{7/2}$ terms to the main $^8S_{7/2}$ term. In other words, within the limits of the $4f^7$ configuration the $V_{so}(Gd^{3+})$ interaction can no longer mix the $[SL]J$ states.

It therefore follows that in the case of a paramagnetic M ion of the Gd^{3+} or Eu^{2+} type the experimentally observed antisymmetric interaction cannot be explained without invoking another mechanism, such as the spin-orbit interaction in the electron shell of the ion with the nucleus N. However, a sufficiently large value of the vector $\mathbf{A}_1$ —representing an electron-nuclear analog of the Dzyaloshinskiĭ-Moriya vector—can be obtained in this case if the ion N is characterized by a strong spin-orbit interaction and sufficiently large electron shells to ensure the effective transfer of the spin density along the Gd^{3+}–O–N chain and a large contribution of the electrons in these shells to the field at the nucleus. All these requirements are satisfied by isoelectronic Pb^{2+} and Be^{3+} ions with an external filled shell $6s^2$ and an empty $6p$ shell of similar energy,[15] and with an anomalously strong spin-orbit coupling (in the case of $6p$ electrons of the Pb^{2+} ion the spin-orbit coupling is $\lambda = 1/2\xi = 0.5$ eV, as given in Ref. 16, and in the case of Bi^{3+} it is even greater). Moreover, these ions are character-

ized by a high electric polarizability, i.e., in a noncentrosymmetric position they exhibit a strong $6sp$ hybridization capable of enhancing the role of both $6s$ and $6p$ electrons in the transfer of the spin density to the relevant nucleus. We must mention also that the antisymmetry effects in the HFS can be detected much more easily for the Pb^{2+} ion than for Bi^{3+}, because the spin of the ^{207}Pb nucleus is $\frac{1}{2}$, whereas in the case of the ^{209}Bi nucleus it is $I = 9/2$, which complicates greatly an analysis of the IHFI due to the need to include the nuclear quadrupole interactions.

An electric field acting on the Pb^{2+} ion can be represented as a sum of two contributions:

$$\mathbf{E}=\mathbf{E}_0+\mathbf{E}_{exch},$$

where $\mathbf{E}_0$ determines the main zero-spin contribution of the crystal environment and of the excess charge of Gd^{3+} to $\mathbf{E}$, whereas $\mathbf{E}_{exch}$ is the spin-dependent part of $\mathbf{E}$ associated with the exchange interaction in the Gd^{3+}-O^{2-}–Pb^{2+} chain. The usual zero-spin contribution $\mathbf{E}_0$ results in mixing of $^1S_0$ and $^1P_1$ states to the ground $6s^2$ and excited $6sp$ configurations, respectively, whereas the exchange contribution E_{exch} mixes the $^1S_0(6s^2)$ state with all the multiplets $^3P_{0,1,2}(6sp)$. In other words, the exchange contribution to the electric field at the Pb^{2+} ion gives rise to electric and magnetic polarization of the $6s^2$ shell.

Calculations carried out on the ground state $6s^2$ of the Pb^{2+} ion allowing for the mixture of the excited states $^1P_1$ and $^3P_{0,1,2}(6sp)$ shows that, to within the terms linear in $\mathbf{E}_0$ and $\mathbf{E}_{exch}$, the effective Hamiltonian of the IHFI in the Ge^{3+}–O^{2-}–$^{207}Pb^{2+}$ chain is

$$\mathcal{H}_{IHFI}=\sum \tilde{A}_k([\hat{E}^{(1)}\otimes e^{(1)}]^{(k)}[\hat{s}^{(1)}\otimes \hat{I}^{(1)}]^{(k)}), \qquad (13)$$

where $\hat{e}^{(1)}$ is a vector parameter governing the exchange part of the electric field exerted by a $Gd^{3+}O^{2-}$ pair on a Pb^{2+} ion and the values of the parameters $\tilde{A}_k$ are determined by the spin-orbit coupling of the $6p$ electron and by the energy structure of the excited states of Pb^{2+}. The components with $k = 0$, 1, and 2 in Eq. (13) describe respectively the isotropic, antisymmetric, and symmetric anisotropic IHFI. It should be noted that without allowance for the spin-orbit coupling in the case of the $6p$ electron, we obtain $\tilde{A}_1 = \tilde{A}_2 = 0$. The nonzero value of the parameter $\tilde{A}_1$ appears if we allow for the effects which are at least linear in respect of V_{so} and it is then found that

$$\tilde{A}_1 \approx -2\lambda \tilde{A}_0/3E(^3P). \qquad (14)$$

The nonzero value of the parameter $\tilde{A}_2$ appears only if we include the effects which are at least quadratic in respect of $V_{so}(6p)$. Therefore, if V_{so} is relatively small ($\lambda \sim 0.5$ eV) compared with the energy of the $6s$-$6p$ transition (it is reported in Ref. 15 that $\Delta E \sim 3$ eV), the parameters of the IHFI in the Gd^{3+}–O^{2-}–$^{207}Pb^{2+}$ chain obey the relationship[1]

$$|A_0| = |A_s| > |\mathbf{A}_1| > A_{zp}^{cov} \sim A_p\eta.$$

It is interesting to note that back in 1968 Schneider[17] demonstrated phenomenologically the appearance of an antisymmetry of the tensor representing the magnetic screening of the nuclei in a model system comprising polarizable and rigid magnetic dipoles in an external magnetic field, showing that the antisymmetric and symmetric anisotropic parts of the magnetic screening tensor are of the same order of magnitude.

We can readily see a considerable similarity between the model system of Schneider and the system for which we observed experimentally the antisymmetric IHFI. In fact, the magnetic moments of the ^{207}Pb nucleus and of the electron shell of the $^{207}Pb^{2+}$ ion are, respectively, rigid and polarizable magnetic moments, whereas the unpaired spin density of Gd^{3+} transferred via O^{2-} is the source of the external magnetic field. The exchange polarization creates a magnetic moment in the Pb^{2+} shell and induces a hyperfine magnetic field at the nucleus of this ion. Finally, in agreement with the predictions of the Schneider model, the antisymmetric and anisotropic symmetric interactions are of the same order of magnitude in our case.

This mechanism of the Gd^{3+}–O^{2-}–$^{207}Pb^{2+}$ indirect hyperfine interaction makes contributions to all the parameters of the effective IHFI interaction and it is found that

$$A_0=\tilde{A}_0\mathbf{E}_0\mathbf{e}/3, \quad \mathbf{A}_1=-\tilde{A}_1[\mathbf{E}_0\times\mathbf{e}]/2, A_{2q}=\tilde{A}_2[\hat{E}_0^{(1)}\otimes\hat{e}^{(1)}]_q^{(2)}. \qquad (15)$$

Therefore, the parameters A_0, $\mathbf{A}_1$, and A_{2q} are not only governed by the magnitude of $\tilde{A}_{0,1,2}$, and by the electric fields $|\mathbf{E}|$ and $|\mathbf{e}|$, but also depend strongly on the relative directions of the vectors $\mathbf{E}$ and $\mathbf{e}$. The electric fields $\mathbf{E}_0$ and $\mathbf{e}$ acting on the Pb^{2+} ion are governed by the position of this ion in a unit cell, as well as by the positions of the Gd^{3+} impurity ion and of the compensator, and by the geometry of the Gd^{3+}–O^{2-}–Pb^{2+} exchange coupling. The last factor affects particularly the magnitude and direction of the exchange part of the electric field $\mathbf{e}$. If we ignore the π bonds, we can represent the vector $\mathbf{e}$ in the form $\mathbf{e} = \mathbf{e}_1\mathbf{r}_{PbO}$, where $e_1 \sim (b_{ss} + b_{\sigma\sigma}\cos\theta)(b'_{ss} + b'_{\sigma\sigma}\cos\theta)$, $\mathbf{r}_{PbO}$ is a unit vector along the Pb^{2+}–O^{2-} bond, b_{ss} and $b_{\sigma\sigma}$ are the effective (hopping) integrals representing the transfer from the $6s$ shell of Pb^{2+} to the $4f$ shell of Gd^{3+}, b'_{ss} and $b'_{\sigma\sigma}$ are the effective hopping integrals representing the transfer from the $4f$ shell of Gd^{3+} to the $6p$ shell of Pb^{2+}, and θ is the angle of the Gd^{3+}–O^{2-}–Pb^{2+} bond. It should be noted that the transfer parameters considered only allowing for just the s or the σ cation-anion bonds, b_{ss} (b'_{ss}) or $b_{\sigma\sigma}$ ($b'_{\sigma\sigma}$), have the same signs and obey the usual inequality $|b_{ss}| < |b_{\sigma\sigma}|$. We can consequently expect the quadratic dependence $e_1(\cos\theta)$ to have two characteristic compensation points (where the value of $\mathbf{e}_1$ vanishes):

$$\cos\theta' = -b_{ss}/b_{\sigma\sigma}, \quad \cos\theta'' = -b_{ss}'/b_{\sigma\sigma}'.$$

It is important to note that the "angular" compensation of the vector $\mathbf{e}$ results, in accordance with Eq. (15), in simultaneous vanishing of all the parameters A_0, $\mathbf{A}_1$, and A_{2q}. The presence of compensation points θ' and θ'' not only alters the magnitude, but can also reverse the signs of the IHFI parameters in the angular range 90–180°.

The ^{207}Pb nuclei, for which we determined the IHFI, are components of Gd^{3+}–O^{2-}–Pb^{2+} chains characterized not only by different bond angles θ and different spatial distributions in the $Pb_5Ge_3O_{11}$ lattice, but also by different lengths of the Gd^{3+}–O^{2-} and $^{207}Pb^{2+}$–O^{2-} bonds. The geometry of the bonds between the nearest ^{207}Pb nuclei (I–V) is demonstrated in Fig. 1 on the basis of the data of Refs. 18

and 19. (We are assuming that, firstly, the structural data obtained for an impurity-free lead germanate lattice at room temperature are sufficient for our qualitative estimates and, secondly, that we need consider only one type of structure of the intermediate O^{2-} ions.)

The dependences of the IHFI parameters on the bond angle θ can be found by normalizing them first and eliminating the dependence on the anion-cation bond length. In qualitative estimates we shall assume that the dependence of the parameter A_s for a Gd^{3+}–O^{2-}–$^{207}Pb^{2+}$ chain on the bond lengths is the same for Gd^{3+}–O^{2-} and $^{207}Pb^{2+}$–O^{2-} and can be approximated by a power law R^{-n} where $n \sim 10$–14 (Ref. 20). Then, selecting as the reference value the bond length in the chain for Pb5 (Fig. 1), we obtain the renormalization coefficients δ for four types of nuclei Pb2, Pb3, Pb5, and Pb6 ($A_s^{norm} = \delta A_s^{exp}$).[2] If $n = 12$, we find that $\delta(Pb2) \approx 0.1$; $\delta(Pb3) \approx 0.3$; $\delta(Pb5) = 1$; $\delta(Pb6) \approx 5$. The experimental values of A_s per one bond are as follows for the nuclei under consideration: $A_s(I) = 725.6$ kHz; $A_s(II) = 5.7$ kHz; $A_s(IV) = -492.1$ kHz. $A_s(V) \approx -133$ kHz (these values are obtained allowing for the fact that the IHFI of the IV and V nuclei involves three equivalent chains). The pairwise attribution of the I and II nuclei to the specific structure types of ^{207}Pb (Pb2 and Pb3) can be made by comparing the experimentally determined angles γ governing the azimuthal orientation of the system of principal axes of the IHFI and structure angles calculated from the data of Refs. 18 and 19 (on the assumption that the ferroelectric distortion of the structure at room temperature is only enhanced by cooling to helium temperature), as shown in Fig. 4. There is no phenomenological criterion for the pairwise identification of the axial nuclei IV and V with the Pb5 and Pb6 nuclei, so that Fig. 4 shows both possible combinations. It is clear from this figure that, in spite of ambiguity in the identification of the axial nuclei, the model considered by us describes correctly the main features of the angular dependence $A_s(\theta)$, particularly the reversal of the sign and the rise of $|A_s|$ on transition across $\theta = 90°$ to smaller angles.

Identification of the nuclei I and II carried out in this way makes it possible to estimate the pseudodipole contribution of the short-range interaction $A_p' = A_p - A_d$. In view of the absence of low-temperature structural data, we shall use A_d calculated from the results of Refs. 18 and 19:

$$A_p'(Pb3) = A_p(I) - A_d(Pb3) = -25.4 \text{ kHz},$$
$$A_p'(Pb2) = A_p(II) - A_d(Pb2) = -5.6 \text{ kHz}.$$

Therefore, it follows from the above description that small values of the parameters A_s and A_p' in the absence of the antisymmetric IHFI in the case of the II nucleus, considered on the basis of the model proposed by us, are related to the angular compensation of the exchange part of the electric field exerted by the Gd^{3+} ion on the Pb^{2+} ion in the Pb2 position, which occurs at $\theta \approx 125°$.

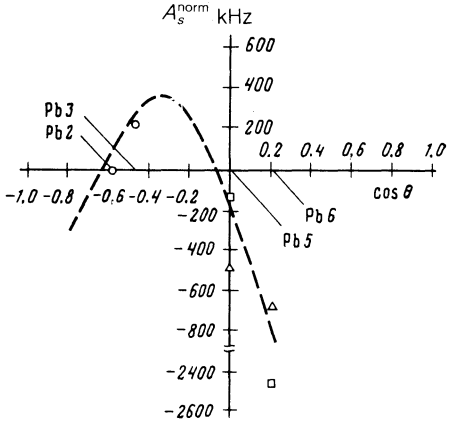

FIG. 4. Qualitative illustration of the dependences of the normalized parameter A_s on the bond angle in a Gd^{3+}–O^{2-}–Pb^{2+} chain; the triangles and squares represent two possible variants of identification of the nuclei III and IV.

5. CONCLUSIONS

The experiments described in the present paper demonstrate that the antisymmetric contribution to the IHFI tensor may give rise to clear experimental manifestations. The strong antisymmetry of the electron-nuclear interaction, which makes such experimental observations possible, can be explained by a strong spin-orbit interaction and a strong $6sp$ hybridization in the electron shell of the Pb^{2+} ion, which in the IHFI case results in electric and magnetic polarizations of the ion. Another manifestation of the $6sp$ hybridization, exhibited by the odd components of the crystal field and by the field of the excess charge of Gd^{3+} at the Pb^{2+} position, is the large paramagnetic component of the screening of the ^{207}Pb nuclei, which appears in experiments as significant variation of the effective nuclear gyromagnetic ratio γ_n as a function of the position of the nucleus in a crystal. Consequently, observation of the antisymmetric IHFI of the nuclei should be easiest in the series of the nuclei exhibiting a large chemical shift in NMR. We can also expect a considerable dependence of the degree of the sp hybridization and, consequently, of the antisymmetric IHFI on the ratio of the charges of the substituting and substituted ions. It would therefore be of considerable interest to investigate the nature of the IHFI of the Eu^{2+} ion in lead germanate. A comparison of the IHFI for isoelectronic Gd^{3+} and Eu^{2+} ions differing in respect of the nuclear charge but present in the same matrix can give information on the relative importance of the contributions to the antisymmetric IHFI made by the electric field of an impurity with a different charge and by the odd components of the crystal field acting on the ions which are at noncentrosymmetric positions in low-symmetry lattices.

We shall conclude by noting that the anomalously strong spin-orbit interaction of the $6p$ electrons of Pb^{2+} or of the isoelectronic Bi^{3+} ions is manifested also by a strong increase of the magnetooptic activity of some magnetic crystals doped with these ions.[21] This may also be useful in the search for the ions promising for the observation of a strong Dzyaloshinskiĭ-Moriya electron-nuclear interaction.

[1)] We are assuming that for $A_p \approx A_d$, where A_d is the parameter of the point dipole interaction, the value of η is a measure of the exchange contribution to the symmetric anisotropic interaction.

[2)] A nucleus of the structure type Pb7 is ignored because, clearly, its IHFI occurs via several intermediate O^{2-} ions, whose contributions are comparable.

[1]S. A. Al'tshuler and V. M. Kozyrev, Electron Spin Resonance of Intermediate-Group Elements [in Russian], Nauka, Moscow (1972), 3.13.

[2]I. E. Dzyaloshinskiĭ, Zh. Eksp. Teor. Fiz. **32**, 1547 (1957) [Sov. Phys. JETP **5**, 1259 (1957)].
[3]T. Moriya, Phys. Rev. **120**, 91 (1960).
[4]V. I. Ozhogin, Author's Abstract of Doctoral Thesis [in Russian], Moscow (1974).
[5]M. L. Meĭl'man and M. I. Samoĭlovich, Introduction to ESR Spectroscopy of Activated Single Crystals [in Russian], Atomizdat, Moscow (1977), Chap. 4.
[6]U. Haeberlen, *High Resolution NMR in Solids*, Academic Press, New York (1976); M. Mehring, *High-Resolution NMR Spectroscopy of Solids*, Springer Verlag, Berlin (1976).
[7]J. M. Baker E.R. Davies, and J. P. Hurrell Proc. R. Soc. A **308**, 403 (1968).
[8]B. G. Berulava R. I. Mirianashvili, O. V. Nazarova, and T. I. Sanadze, Fiz. Tverd. Tela (Leningrad) **19**, 1771 (1977) [Sov. Phys. Solid State **19**, 1033 (1977)].
[9]P. M. Levy J. Appl. Phys. **40**, 1139 (1969) (Proc. Fourteenth Annual Conf. on Magnetism and Magnetic Materials, New York (1968)].
[10]A. I. Rokeakh, N. V. Legkikh, Yu. A. Sherstkov, and A. E. Sibiryakov, Fiz. Tverd. Tela (Leningrad) **26**, 151 (1984) [Sov. Phys. Solid State **26**, 88 (1984)].
[11]A. I. Rokeakh, N. V. Legkikh, and Yu. A. Sherstkov, Deposited Paper No. 7574-V.Dep [in Russian], VINITI, Moscow (1985).
[12]A. Abragam and B. Bleaney, *Electron Paramagnetic Resonance of Transition Ions*, Clarendon Press, Oxford (1970).
[13]G. E. Forsythe, M. A. Malcolm, and C. B. Moler, *Computer Methods for Mathematical Computations*, Prentice-Hall, Englewood Cliffs, N.J. (1977).
[14]A. S. Moskvin, Author's Abstract of Doctoral Thesis [in Russian], Moscow (1984).
[15]H. Ito, H. Onuki, and R. Onaka, J. Phys. Soc. Jpn. **45**, 2043 (1978).
[16]E. Goovaerts, S. Nistor, and D. Schoemaker, Phys. Rev. B **25**, 83 (1982).
[17]R. F. Schneider, J. Chem. Phys **48**, 4905 (1968).
[18]Y. Iwata, N. Koyano, I. Shibuya, N. Niizeki, and H. Koizumi, J. Phys. Soc. Jpn **35**, 324 (1973).
[19]M. I. Kay, R. E. Newnham, and R. W. Wolfe, Ferroelectrics **9**, 1 (1975).
[20]J. M. Baker, J. Phys. C **12**, 4039 (1979).
[21]J. F. Dillon Jr, Proc. Third Intern. Conf. on Ferrites, Kyoto, 1980, publ. by Reidel, Dordrecht, Netherlands (1982), p. 743.

Translated by A. Tybulewicz